USGS
science for a changing world

Studies by the U.S. Geological Survey in Alaska, 2010

Constraining the Age and Magnitude of Uplift in the Northern National Petroleum Reserve in Alaska (NPRA)—Apatite Fission-Track Analysis of Samples from Three Wells

Professional Paper 1784-A

U.S. Department of the Interior
U.S. Geological Survey

Cover.— Northeastern NPRA coastal plain with meandering stream and thermokarst lakes. Field of view in middle of photo is approximately 1/2 mile. Location in northeastern National Petroleum Reserve in Alaska (NPRA) about 20 miles west of Colville River delta.

Studies by the U.S. Geological Survey in Alaska, 2010

Constraining the Age and Magnitude of Uplift in the Northern National Petroleum Reserve in Alaska (NPRA)—Apatite Fission-Track Analysis of Samples from Three Wells

By David W. Houseknecht, Kenneth J. Bird, and Paul O'Sullivan

Professional Paper 1784-A

U.S. Department of the Interior
U.S. Geological Survey

U.S. Department of the Interior
KEN SALAZAR, Secretary

U.S. Geological Survey
Marcia K. McNutt, Director

U.S. Geological Survey, Reston, Virginia: 2011

This report and any updates to it are available online at:
http://pubs.usgs.gov/pp/1784/a/

For more information on the USGS—the Federal source for science about the Earth, its natural and living resources, natural hazards, and the environment, visit http://www.usgs.gov or call 1-888-ASK-USGS (1-888-275-8747).

For an overview of USGS information products, including maps, imagery, and publications, visit http://www.usgs.gov/pubprod

To order this and other USGS information products, visit http://store.usgs.gov

Suggested citation:
Houseknecht, D.W., Bird, K.J., and O'Sullivan, Paul, 2011, Constraining the age and magnitude of uplift in the northern National Petroleum Reserve in Alaska (NPRA)—apatite fission-track analysis of samples from three wells, *in* Dumoulin, J.A. and Dusel-Bacon, Cynthia, eds., Studies by the U.S. Geological Survey in Alaska, 2010: U.S. Geological Survey Professional Paper 1784-A, 21 p. 1 plate.

Contents

Plate

Figures

Tables

This page left blank intentionally.

Studies by the U.S. Geological Survey in Alaska, 2010
Edited by Julie A. Dumoulin and Cynthia Dusel-Bacon
U.S. Geological Survey Professional Paper 1784-A

Constraining the Age and Magnitude of Uplift in the Northern National Petroleum Reserve in Alaska (NPRA)—Apatite Fission-Track Analysis of Samples from Three Wells

By David W. Houseknecht[1], Kenneth J. Bird[2], and Paul O'Sullivan[3]

Abstract

A broad, post-mid-Cretaceous uplift is defined in the northern National Petroleum Reserve in Alaska (NPRA) by regional truncation of Cretaceous strata, thermal maturity patterns, and amounts of exhumation estimated from sonic logs. Apatite fission-track (AFT) analysis of samples from three wells (South Meade No. 1, Topagoruk No. 1, and Ikpikpuk No. 1) across the eastern flank of the uplift indicates Tertiary cooling followed by Quaternary heating.

Results from all three wells indicate that cooling, presumably caused by uplift and erosion, started about 75–65 Ma (latest Cretaceous–earliest Tertiary) and continued through the Tertiary Period. Data from South Meade indicate more rapid cooling after about 35–15 Ma (latest Eocene–middle Miocene) followed by a significant increase in subsurface temperature during the Quaternary, probably the result of increased heat flow. Data from Topagoruk and Ikpikpuk include subtle evidence of accelerated cooling starting in the latest Eocene–middle Miocene and possible evidence of increased temperature during the Quaternary. Subsurface temperature perturbations related to the insulating effect of permafrost may have been responsible for the Quaternary temperature increase at Topagoruk and Ikpikpuk and may have been a contributing factor at South Meade.

Multiple lines of geologic evidence suggest that the magnitude of exhumation resulting from uplift and erosion is 5,000–6,500 ft at South Meade, 4,000–5,500 ft at Topagoruk, and 2,500–4,000 ft at Ikpikpuk. The results from these wells help to define the broad geometry of the uplift, which increases in magnitude from less than 1,000 ft at the Colville River delta to perhaps more than 7,000 ft along the northwestern coast of NPRA, between Point Barrow and Peard Bay. Neither the origin nor the offshore extent of the uplift, west and north of the NPRA coast, have been determined.

Introduction

Seismic and well data collected in the National Petroleum Reserve in Alaska (NPRA; formerly the Naval Petroleum Reserve No. 4) by the U.S. Navy and the U.S. Department of the Interior during two phases of exploration (1944–1953 and 1974–1982) reveal a broad uplift in northern NPRA, the origin of which is poorly understood. The uplift is defined by truncation of Cretaceous strata beneath an unconformity at the base of the Pliocene–Pleistocene Gubik Formation (fig. 1), which forms a thin veneer of surficial sediments across the region. Strata as young as Paleogene (lower Sagavanirktok Formation) lie beneath the unconformity in easternmost NPRA and progressively older strata lie beneath it to the west. The truncation edge of the basal Upper Cretaceous Seabee Formation occurs just west of Teshekpuk Lake (fig. 2). The Lower Cretaceous Nanushuk Formation lies beneath the unconformity everywhere to the west, except near Point Barrow, where the Nanushuk is completely eroded and the uppermost part of the underlying Torok Formation lies beneath the Gubik unconformity (fig. 2).

Information emerging from recent oil-exploration drilling in northern NPRA suggests that the broad uplift described above may have influenced whether oil or gas is found in Jurassic reservoirs (Houseknecht and others, 2010). Uplift and erosion across northern NPRA would have caused a decrease in confining pressure on subsurface fluids, resulting in degassing of oil in reservoirs, expansion of free gas in reservoirs, and degassing of formation water. An abrupt lateral gradation from oil on the east to gas on the west, just 15–20 miles west of the Colville River delta, and a predominance of gas in Jurassic reservoirs everywhere to the west are hypothesized to be the result of these uplift-induced processes.

[1]U.S. Geological Survey, Reston, Va.

[2]U.S. Geological Survey, Menlo Park, Calif.

[3] Apatite to Zircon, Inc. Viola, Idaho.

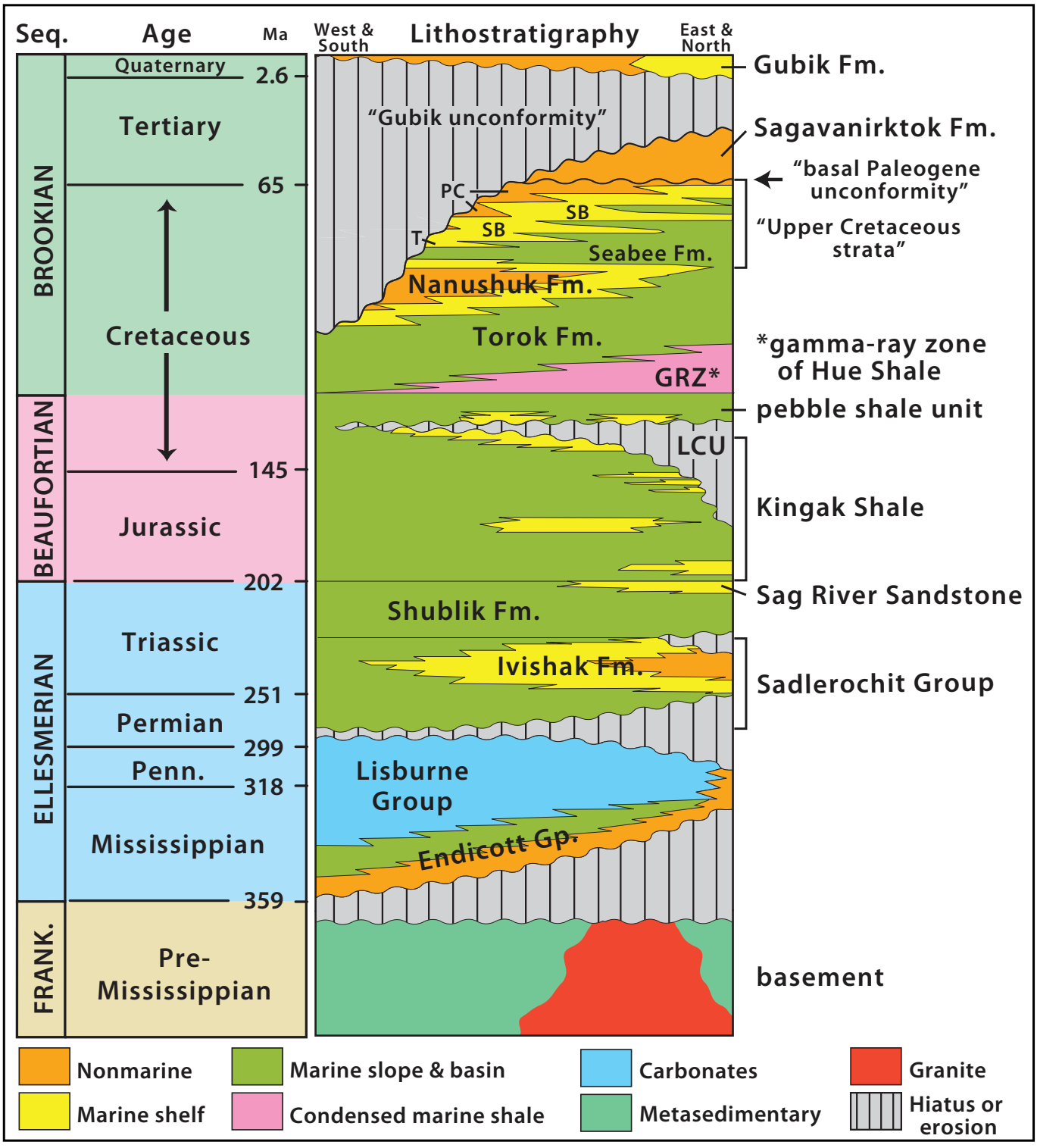

Figure 1. Chronostratigraphy of the National Petroleum Reserve in Alaska showing megasequences at left and lithostratigraphic names at right. Informal terms used in text are shown in quotation marks. Some Upper Cretaceous formation names are abbreviated as follows: PC, Prince Creek; SB, Schrader Bluff; T, Tuluvak; LCU, Lower Cretaceous unconformity; Seq., megasequences; Frank., Franklinian. Stratigraphic column modified from Mull and others (2003) and Houseknecht and Bird (2004); absolute ages from Walker and Geissman (2009).

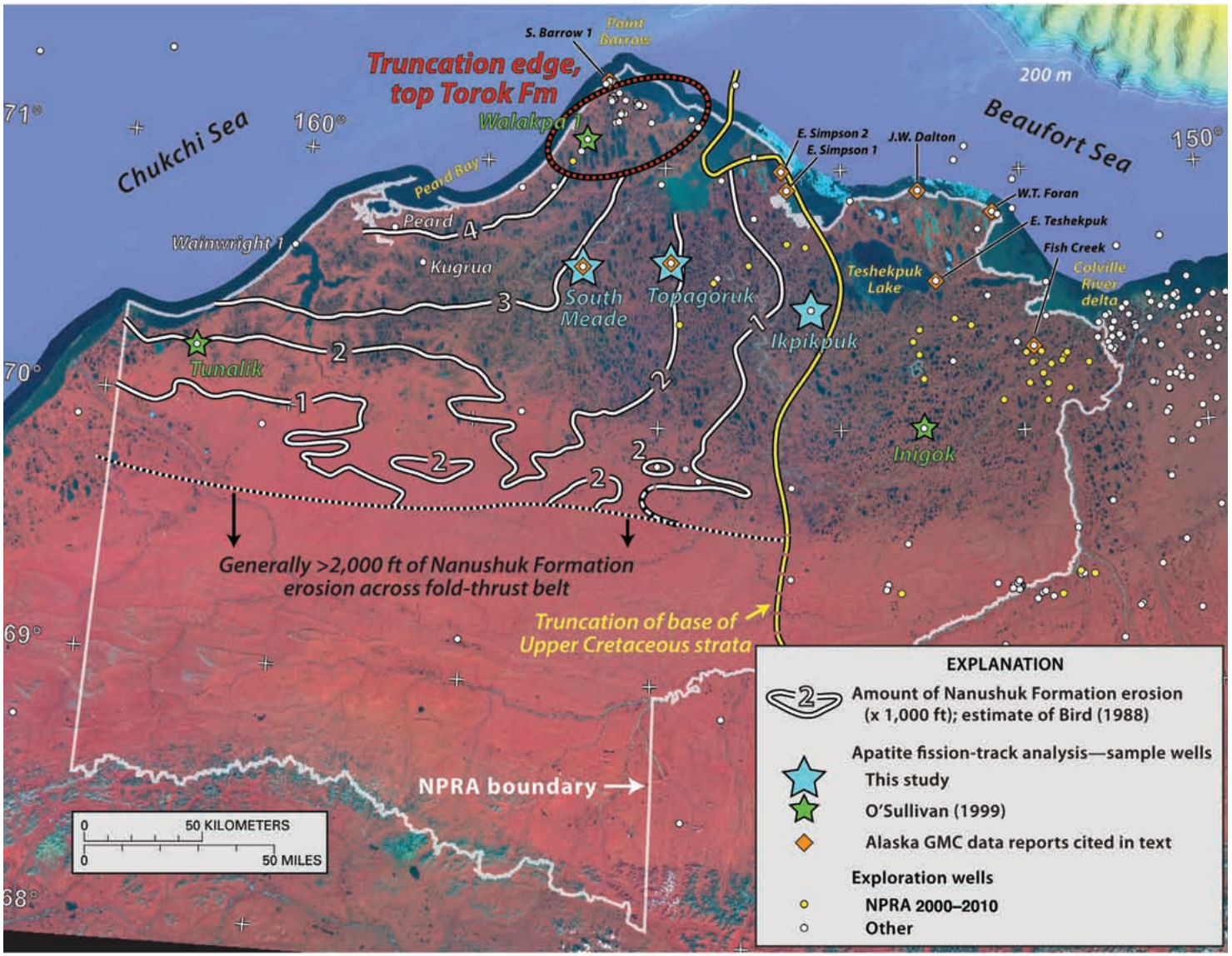

Figure 2. Magnitude of Nanushuk Formation erosion in the National Petroleum Reserve in Alaska (NPRA; boundary shown by white line) with locations of exploration wells, contours (white) of magnitude of Nanushuk Formation erosion (Bird, 1988), and wells for which apatite fission-track data are discussed in this report. Northern extent of Tertiary folding associated with Brooks Range deformation is indicated by pervasive red color in base map, which reflects topographically higher areas covered with tundra, and west-east elongated white contour patterns south of 70° latitude. Red and black dotted line labeled "Truncation edge, top Torok Fm" is the area where the Nanushuk Formation is completely eroded and the uppermost Torok Formation lies beneath the "Gubik unconformity." Map base is a false-color, composite Landsat image.

The U.S. Geological Survey conducted an apatite fission-track (AFT) thermochronologic study on core samples from three exploration wells in northern NPRA to provide additional information that can be used to interpret the history of this uplift. The objective of this paper is to present the results of that study, which constrain the timing and magnitude of uplift and erosion in the vicinity of those wells.

Geologic Background

The general outline of the southern and eastern margins of the northern NPRA uplift was delineated by Bird (1988) using structure-contour and isopach maps of Cretaceous strata (fig. 2). The northern and western margins of the uplift have not been delineated. Bird's (1988) Nanushuk Formation structure-contour map is especially revealing, as it was "restored" across the area of Nanushuk truncation by projection of seismic horizons. The map indicates that the amount of erosion increases to the northwest across NPRA, with more than 4,000 ft of the Nanushuk Formation eroded near the coast between Point Barrow and Peard Bay (fig. 2). Bird's (1988) map also demonstrates that the northern NPRA uplift is distinct from the uplifted frontal fold-thrust belt of the Brooks Range (fig. 2), whose origin is well known (for example, Moore and others, 2004).

Additional geological data document the general outline of the northern NPRA uplift. For example, Johnsson and others (1993) showed that the elevation of the 0.6 percent vitrinite reflectance isopleth increases from about 12,000 ft subsea in the vicinity of the Colville River delta to about 5,000 ft subsea at Point Barrow. Nelson and Bird (2005) used vitrinite reflectance data from several exploration wells in northern NPRA to estimate a westward increase in uplift and erosion, from 1,000 ft or less near the Colville River delta to nearly 7,000 ft between Point Barrow and Peard Bay.

Nelson and Bird (2005) also used sonic logs from exploration wells to characterize compaction trends in the Lower Cretaceous Torok Formation and estimated that uplift and erosion in northern NPRA increase from zero north of the Colville River delta to more than 5,000 ft between Point Barrow and Peard Bay. Burns and others (2007) used an alternative approach to analyze sonic logs from exploration wells and to estimate the amount of uplift and erosion across the entire Alaska North Slope and adjacent offshore areas. They concluded that the amount of uplift and erosion in northern NPRA increases from less than 1,000 ft in the Colville River delta to more than 3,000 ft in the vicinity of Peard Bay (fig. 3).

Although most previous studies involving AFT analysis have focused on the Brooks Range and the associated fold-thrust belt, a few indications of the northern NPRA uplift have emerged from that work. For example, O'Sullivan (1999) documented significant cooling at about 60 Ma in samples from the Walakpa No. 1, Tunalik No. 1, and Inigok No. 1 wells in northern NPRA (figs. 2 and 3). These three wells are north of the fold-thrust belt and do not display evidence of significant structural thickening that would suggest uplift related to folding or thrust faulting. In addition, data reports submitted to the Alaska Geological Materials Center include AFT data for several wells in northern NPRA (Bergman and others, 1991; Murphy, 1994). Although the summary data in these reports are not sufficient to interpret precise cooling histories, they do suggest cooling ages that generally are consistent with post-Cretaceous exhumation for the following wells: South Barrow No. 1, East Simpson No. 1, East Simpson No. 2, J.W. Dalton, W.T. Foran, East Teshekpuk, Fish Creek, South Meade, and Topagoruk (figs. 2 and 3).

All these independent geological parameters indicate the presence of a broad uplift in northern NPRA, although the timing of uplift is poorly constrained and the estimated magnitude of uplift and erosion is widely variable. Nevertheless, all these techniques have produced estimates that consistently indicate an increased magnitude of uplift and erosion westward, from little or no exhumation in the vicinity of the Colville River delta to several thousand feet of exhumation near the northwestern coast of NPRA.

Most previous interpretations of uplift along the northern coast of Alaska have focused on two temporally overlapping events that occurred during the Late Jurassic–Early Cretaceous, convergent tectonism that formed the Brooks Range on the south and uplift of the "Alaska rift shoulder" (Houseknecht and Bird, 2011) during extensional opening of the Canada basin on the north. In this context, uplift along the Barrow arch (the structurally highest part of the rift shoulder at present)—including northern NPRA—has been attributed primarily to rift-shoulder uplift and flexural uplift associated with tectonic loading by the Brooks Range (for example, Nunn and others, 1987; Coakley and Watts, 1991).

Post-Cretaceous uplift in northern NPRA generally has been attributed to eastward tilting of the Beaufort rift shoulder in response to tectonic and sedimentary loading by the northeastern Brooks Range (for example, Hubbard and others, 1987). Coakley and Watts (1991) described the seismic signature of the broad uplift in northern NPRA and suggested that it resulted from the constructive interference of flexural bulges related to crustal loading by the Brooks Range and the Beaufort passive-margin sediment prism.

Samples and Methods

Three exploration wells—South Meade No. 1, Topagoruk No. 1, and Ikpikpuk No. 1—were selected for AFT analysis based on their locations on the eastern flank of the northern NPRA uplift (figs. 2 and 3). The elevations of both the ground surface and the kelly bushing, which is the datum for sample depth measurements, are similar for the three wells (table 1). The reference datum, therefore, can be considered horizontal for purposes of interpreting amount of uplift and erosion.

Samples were collected from conventional cores archived at the U.S. Geological Survey (USGS) Core Research Center in Lakewood, Colorado. Table 1 summarizes essential information, including the depth and approximate temperature and thermal maturity (vitrinite reflectance), for each sample.

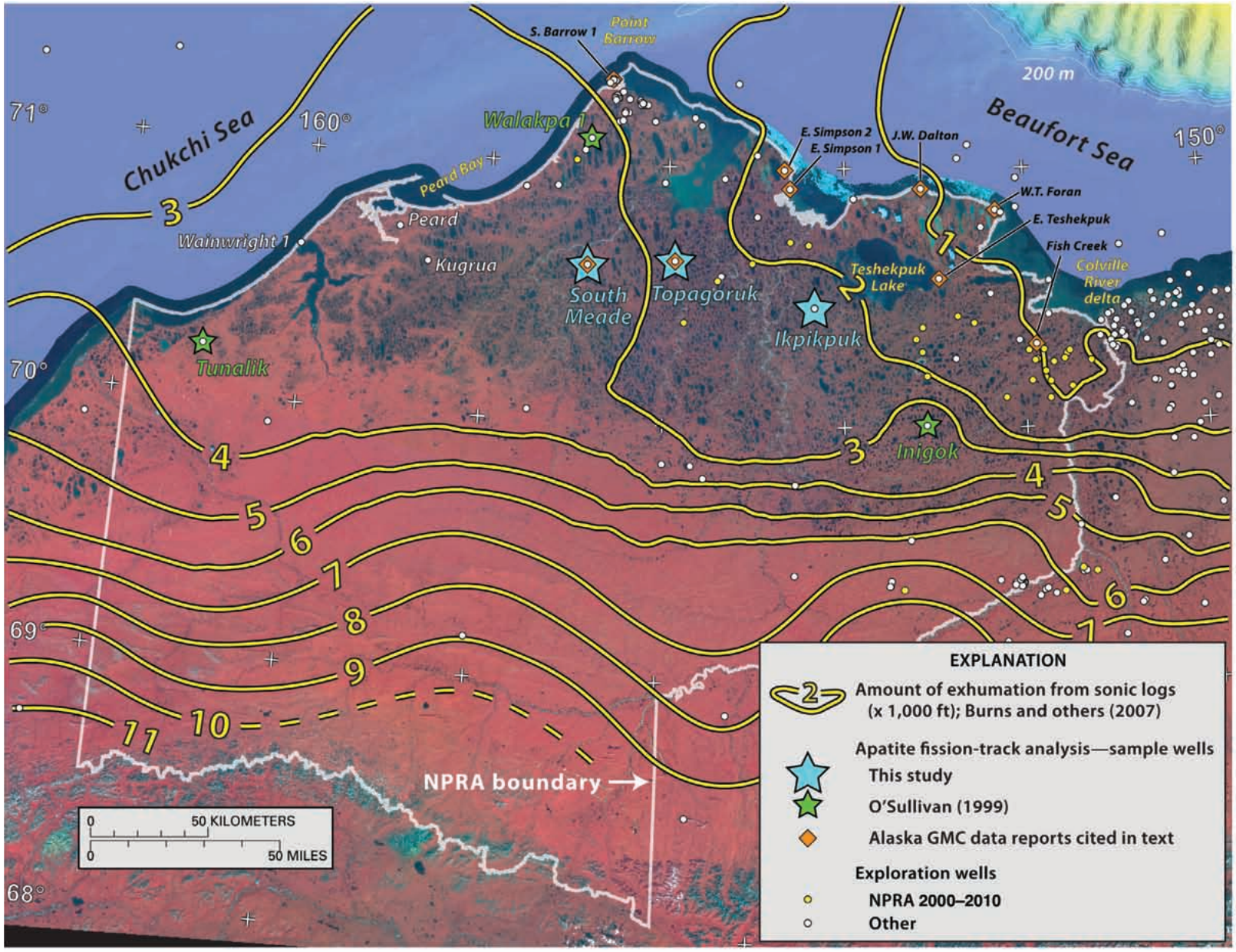

Figure 3. Amount of erosion in the National Petroleum Reserve in Alaska estimated from sonic logs from exploration wells (NPRA; boundary shown by white line) with locations of exploration wells, contours (yellow) of amount of exhumation estimated from sonic logs (Burns and others, 2007), and wells for which apatite fission-track data are discussed in this report. Map base is a false-color, composite Landsat image.

Samples were prepared and analyzed using standard techniques of AFT analysis, as described by Donelick and others (2005). AFT thermochronology provides a record of the thermal history of the host rock below a temperature of about 110°C. Following their formation, fission tracks at surface temperatures retain a relatively constant mean length of about 16 μm over geologic time. With increased temperature, apatite fission tracks are partially annealed above about 60°C and totally annealed above about 110°C (Gleadow and others, 1986; Dumitru, 2000; Donelick and others, 2005). Increased annealing yields shorter fission tracks, apparently lower track density, and reduced fission-track age. Total annealing reduces the fission-track age to zero.

Interpretation of data collected from well samples (tables 1–3) was facilitated by the use of HeFTy (Ketcham, 2005), a quantitative modeling program. HeFTy provides the capability to test alternative time-temperature (t-T) histories for each sample by statistically assessing the goodness of fit between AFT length distributions generated by kinetic modeling of AFT annealing and measured AFT length distributions (Carlson and others, 1999; Donelick and others, 1999; Ketcham and others, 1999, 2000, 2007; Ketcham, 2005).

Chronostratigraphic ages used for modeling are based on Moore and others (1994) and Mull and others (2003) and correlated to absolute ages based on Walker and Geissman (2009).

Geologic Constraints for Time-Temperature Modeling

HeFTy (Ketcham, 2005) was used to model the t-T history of each sample, primarily using the inverse modeling option. Inverse modeling requires the input of t-T constraints, each of which consists of a range of time and temperature representing geologic conditions to which the sample was exposed. Constraints used for modeling the South Meade, Topagoruk, and Ikpikpuk samples were defined by using well-established stratigraphy and geologic history, as well as the output of previous thermal maturation modeling (Houseknecht and others, in press). These constraints are described below, are summarized in table 4, and are shown as lettered rectangles on the t-T plots in plate 1.

Provenance ("P" in plate 1).—This constraint represents the high temperature (well above that required for total annealing) source of apatite found in each sample; a nominal temperature range of 200–220°C, well above the total annealing temperature of apatite, was used for all provenance constraints (table 4). Significantly, most samples during Cretaceous burial were exposed to temperatures within or above the apatite partial or total annealing temperature windows, so the rather generic ranges of time and temperature specified for the provenance constraints exert little or no influence on modeling outcomes. Nevertheless, these constraints were used to honor a consistent modeling approach that includes provenance terrane. Provenance for Brookian strata (Torok and Nanushuk Formations; fig. 1) is considered to be the Chukotka and Brooks Range orogenic belts, whose rocks were uplifted from great depths and temperatures during Late Jurassic–Early Cretaceous tectonism (Houseknecht and Bird, 2011). Accordingly, a time range of 150–120 Ma was used for samples from South Meade and Topagoruk, and a time range of 150–115 Ma was used for samples from Ikpikpuk. The slightly younger minimum age was used for Ikpikpuk samples to reflect the time-transgressive nature of the Early Cretaceous depositional system (Houseknecht and others, 2009) and the corresponding possibility of younger apatite provenance. Provenance for the Ivishak, Shublik, Sag River, and Kingak Formations (fig. 1) is considered to be the pre-Mississippian Franklinian basement, broadly deformed during the Late Devonian—Early Mississippian Ellesmerian orogeny (Moore and others, 1994), and for which a time range of 350–250 Ma was used (table 4). One sample (TK-7) of pre-Mississippian basement required a provenance age older than the Ellesmerian orogeny, and a time range of 500–370 Ma was used.

Deposition ("D" or "X" in plate 1).—This constraint represents exposure of apatite to surface or near-surface temperatures during transport and deposition within a sedimentary system and shallow burial following deposition. A temperature range of 5–20°C was used for all samples. Time constraints (table 4) are based on the age of the formation, sample position within the formation (near base, near middle, near top) and, in the case of Torok and Nanushuk samples, the time transgressive nature of the depositional system (Houseknecht and others, 2009). In the case of the basement sample (TK-7), from an anomalous sedimentary section in what is otherwise a regionally low-grade metamorphic basement, the time range is an estimate of when the sample may have been near surface exposure prior to the onset of Ellesmerian sedimentation ("X" in plate 1).

Neocomian burial ("N" in plate 1) and rift-shoulder uplift ("R" in plate 1).—These constraints represent (1) burial of each sample older than the Lower Cretaceous unconformity (LCU; fig. 1) to the highest temperature reached prior to (2) rift-shoulder uplift associated with opening of the Canada Basin and resultant erosional exhumation to form the LCU (fig. 1). Time constraints used for Neocomian burial and rift-shoulder uplift are 136–133 Ma and 133–128 Ma, respectively. The ranges of temperature to which each sample was exposed during these events initially were estimated from the output of geohistory modeling constrained by vitrinite reflectance (VR) data (Houseknecht and others, in press) and, ultimately, were expanded to account for uncertainty in VR and AFT measurement and interpretation, as well as the results of initial modeling outcomes. These temperature constraints are summarized in table 4.

Early Cretaceous burial ("E" in plate 1) and Late Cretaceous–Earliest Tertiary burial ("T" in plate 1).—These constraints represent burial by Lower Cretaceous through basal Tertiary strata of the Brookian Sequence (fig. 1). Two discrete constraints were used, rather than one, to reflect the more rapid sediment accumulation during the Early Cretaceous as compared to the Late Cretaceous and earliest Tertiary.

Time constraints (table 4) are based on the age of the formations (Mull and others, 2003), sample position within the formations, and the time-transgressive nature of the Early Cretaceous depositional system (Houseknecht and others, 2009). Temperature constraints were estimated from geohistory modeling (Houseknecht and others, in press) and were expanded to account for uncertainty regarding the original presence and thickness of Upper Cretaceous and basal Tertiary strata, neither of which are present in the sample wells, and the results of initial modeling outcomes. These temperature constraints are summarized in table 4.

Pliocene–Pleistocene low temperature ("L" in plate 1).—This is the only constraint that was not specified prior to modeling. The addition of this constraint became necessary during modeling of 12 of the 19 samples to achieve an optimal match between measured AFT length distributions and model results. The time and temperature constraint ranges were established using the forward modeling capability of HeFTy (Ketcham, 2005).

Current temperature ("C" in plate 1).—The current temperature (table 1) for each sample was derived from geothermal gradients estimated from corrected bottom-hole temperature measurements (for example, Deming and others, 1992). For inverse modeling purposes, a temperature constraint centered on the current temperature with a ±5°C range was set at a time of 0 Ma (table 4).

Results

AFT data were collected from 19 samples, six from South Meade, seven from Topagoruk, and six from Ikpikpuk. Data and interpretations are summarized in tables 1–3, figures 4 and 5, and plate 1. The following sections provide a summary of data and interpretations for samples from each well.

South Meade No. 1

South Meade is on the eastern flank of the northern NPRA uplift in an area where Bird (1988) estimated approximately 3,000 ft of Nanushuk erosion (fig. 2). The South Meade well is distinct for its thermal maturity, geothermal gradient, and heat flow—all of which are among the highest measured in NPRA exploration wells (Deming and others, 1992, 1996; Houseknecht and others, in press). Samples range in stratigraphic position from the Triassic Ivishak Formation, at 9,253 ft subsea (elevation) and a vitrinite reflectance of 2.3 percent, to the Lower Cretaceous Torok Formation, at 2,958 ft subsea and a vitrinite reflectance of 0.6 percent (table 1).

Samples SM-6 through SM-3 currently are at temperatures above the threshold of total AFT annealing (≈110°C), SM-2 is within the temperature window of partial annealing (≈60-110°C), and SM-1 is at a temperature clearly below the partial annealing threshold (table 1; fig. 4). There is a systematic increase in the number and mean length of fission tracks up section (fig. 4). Samples SM-6 and SM-5 contain so few fission tracks that they are interpreted to represent nearly total annealing. Up section, the number of fission tracks increases in SM-4, and even more so in SM-3 and SM-2 (fig. 4), suggesting that these samples represent the transition from the total-annealing to the partial-annealing temperature windows. SM-1 contains the largest number of fission tracks, as well as the largest mean track length among samples from this well (fig. 4).

The age of the oldest fission tracks and the pooled fission-track age both generally increase up section (fig. 5). The age of oldest tracks increases from 0.0 to 23.5 Ma over just 800 ft of stratigraphic section from SM-6 to SM-3, then increases slightly over 2,500 ft of section to 26.1 Ma in SM-2 (fig. 5). The pooled AFT age, which closely tracks the oldest track age (fig. 5), suggests that cooling continued at least until the latest Tertiary (≈7–5 Ma). Sample SM-1, whose AFT data are interpreted on the basis of *D*par (diameter of etch figures parallel to the crystallographic c axis; Donelick and others, 2005) measurements to represent two populations (table 1; fig. 5), yielded ages of 78.5 and 108 Ma for the oldest tracks in the sample (fig. 5). The former may represent tracks formed during shallow burial following deposition and not completely annealed during subsequent burial, or it may reflect the earliest phase of uplift following maximum burial, whereas the latter likely represents tracks formed during uplift of the provenance terrane, sediment dispersal, and deposition.

Although the data discussed above suggest ongoing annealing of apatite in samples SM-6 through SM-3 and partial annealing in SM-2, the retention of fission tracks, especially in samples SM-5 through SM-3, at temperatures 10–25°C higher than the threshold temperature for total annealing (table 1) suggests that these samples were exposed to current temperature for a short time. Time-temperature modeling suggests that all South Meade samples must have been exposed to lower-than-current temperatures followed by a significant increase in temperature within the past 2 million years (plate 1).

Time-temperature modeling of South Meade samples suggests a somewhat complex Cenozoic cooling history. The t-T model for SM-1 suggests a monotonic cooling history that started around 75–65 Ma and continued until the Quaternary (plate 1). The oldest track that appears to post-date deposition (78.5 ±6.3 Ma) could have formed during shallow burial and been subjected to partial annealing during deeper burial or, considering the younger end of the uncertainty range, could reflect initial cooling at 72.2 Ma.

The t-T models for SM-2 through SM-4 provide the best indication of cooling history. Those three models suggest relatively slow cooling from 75–65 Ma to the mid-Cenozoic followed by relatively rapid cooling to the Quaternary (plate 1). Specifically, the t-T models for SM-2 and, to a lesser extent, SM-3 suggest accelerated cooling starting at 35–30 Ma, whereas the models for SM-3 and SM-4 suggest accelerated cooling starting at 25–15 Ma (plate 1). The oldest tracks in these three samples (SM-2, 26.1 Ma; SM-3, 23.5 Ma; and

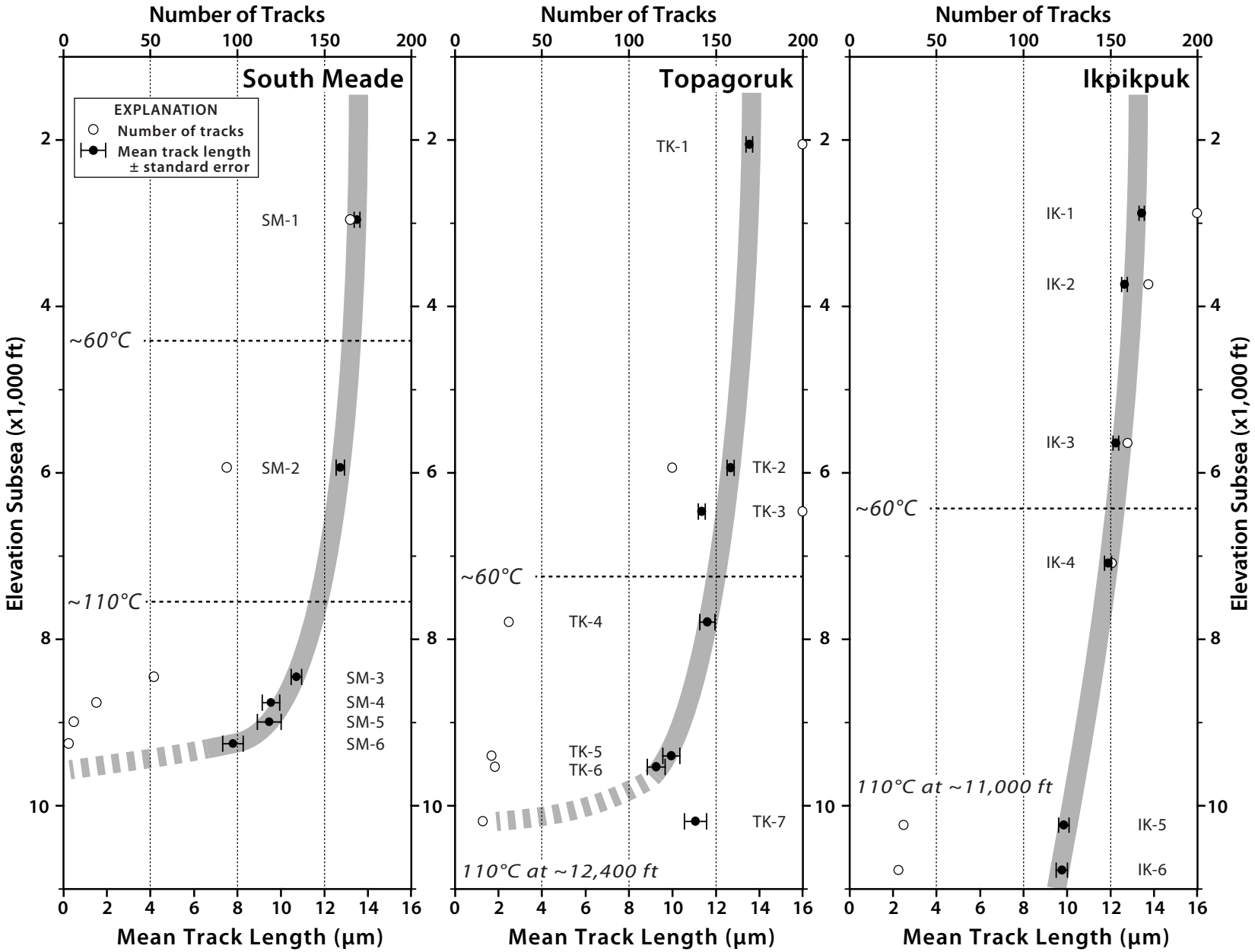

Figure 4. Plots of elevation versus number of apatite fission tracks and mean track length in samples from each analyzed well. Inferred apatite fission-track annealing curves are indicated by broad, gray lines. Approximate temperature thresholds of partial (≈60°C) and total (≈110°C) annealing were determined using current surface temperature (from Lachenbruch and others, 1988) and estimates of current geothermal gradient (table 1).

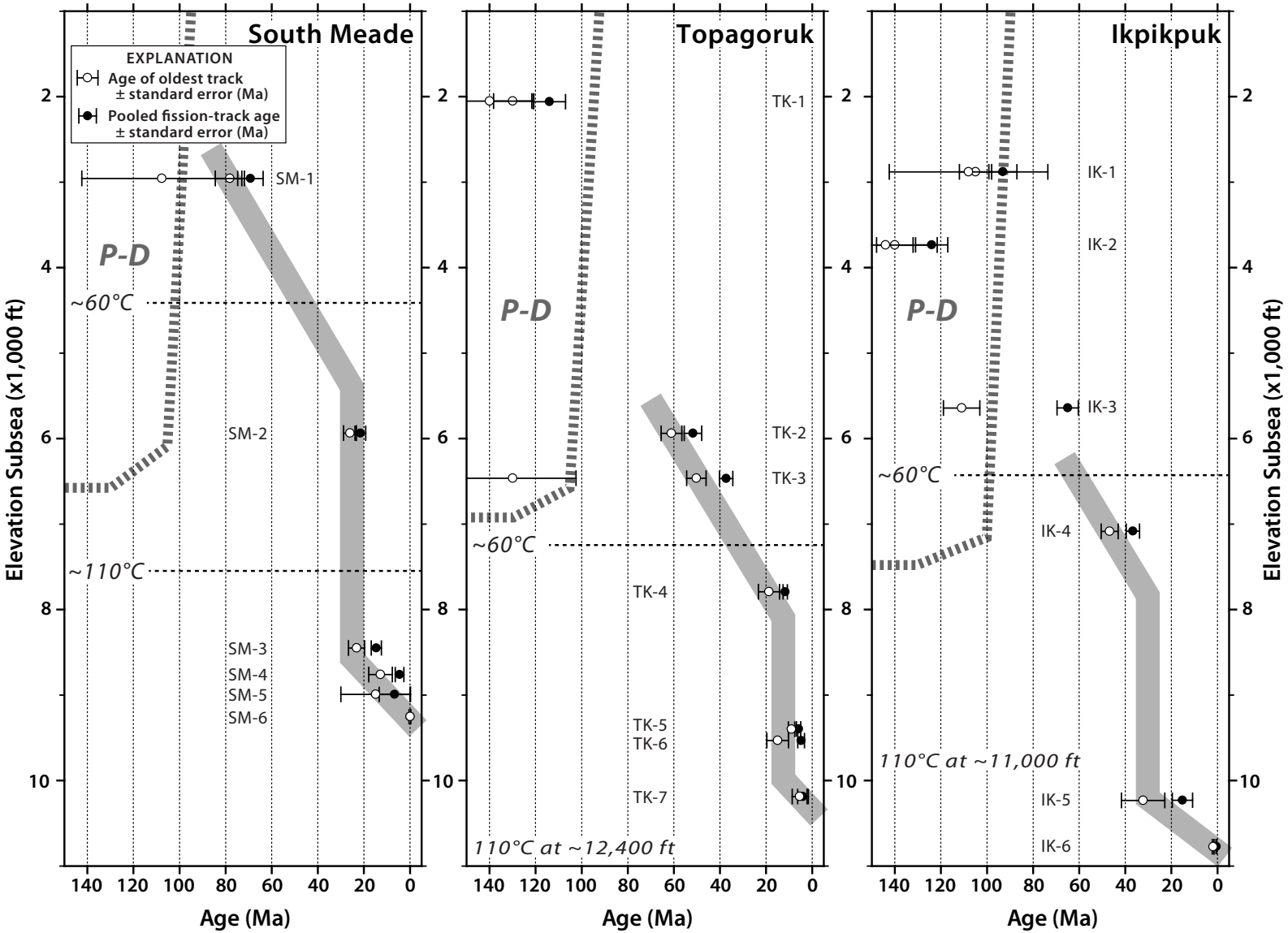

Figure 5. Plots of elevation versus age of oldest apatite fission track and pooled fission-track age for each analyzed well. Broad, gray lines indicate trends of elevation versus oldest fission track; vertical portion of gray line is interpreted to indicate accelerated uplift; width of gray line is approximately 10 million years. Gray dashed line in each plot represents elevation of strata in well bore versus approximate age of those strata, and an AFT age that plots within the area labeled P-D is older than the stratigraphic unit from which the sample was collected. Thus, an AFT age that plots within the P-D field represents fission-track formation during uplift and cooling of provenance terrane, residence within sediment dispersal and depositional system, or shallow burial following deposition. Approximate temperature thresholds of partial (≈60°C) and total (≈110°C) annealing are the same as those in fig. 4.

SM-4, 12.7 Ma; table 1, fig. 5), as well as the population of tracks represented by the pooled AFT age (table 2), would have formed during the accelerated cooling trajectory suggested by the t-T models.

SM-5 and SM-6 provide limited insights regarding the timing of the northern NPRA uplift because both samples have been in the partial or total apatite annealing windows during most of the Cenozoic, although the 15.1 Ma age of the oldest track in SM-5 may corroborate the interpretation of an accelerated cooling trajectory during the Late Cenozoic. Inferences based on t-T modeling of these two samples are tentative because their long residence time in the total annealing zone results in a very broad envelope of statistically good fits to the measured AFT length data (plate 1).

Vitrinite reflectance values calculated using the "Easy $\%R_o$" kinetics of Sweeney and Burnham (1990) compare favorably with values derived from measured vitrinite reflectance for all six t-T models (table 4; plate 1). This comparison provides corroboration that the t-T models are reasonable approximations of the thermal history of each sample.

Topagoruk No. 1

Topagoruk is at an intermediate position on the eastern flank of the northern NPRA uplift in an area where Bird (1988) estimated approximately 2,000 ft of Nanushuk erosion (fig. 2). Topagoruk is in an area of moderate heat flow, as estimated by regional analysis (Deming and others, 1992, 1996). Samples range in stratigraphic position from the pre-Mississippian basement, at 10,187 ft subsea and a post-Mississippian thermal maturity of approximately 1.2 percent vitrinite reflectance (see below), to the Lower Cretaceous Nanushuk Formation, at 2,051 ft subsea and a vitrinite reflectance of 0.5 percent (table 1). In contrast to low-grade metamorphic argillite that is predominant across northern NPRA, basement rocks penetrated by the Topagoruk well are sedimentary strata in which measured mean vitrinite reflectance varies nonsystematically relative to depth from 1.07 to 1.50 percent over a 300 ft depth interval (Johnsson and others, 1999); the measured value nearest the AFT sample is 1.19 percent.

Samples TK-7 through TK-4 currently are at temperatures within the partial AFT annealing window, TK-3 and TK-2 are at temperatures slightly lower than the threshold of partial annealing, and TK-1 is at a temperature well below the threshold of partial annealing (fig. 4). Samples TK-7 through TK-4 contain few tracks, whereas TK-3 through TK-1 contain abundant tracks, and the mean track length generally increases up section (fig. 4). Exceptions to this general trend include a sedimentary basement sample (TK-7), whose mean track length is larger than two shallower samples, and TK-3, whose mean track length is shorter than the next deeper and shallower samples (fig. 4). These observations suggest that samples TK-7 through TK-4 have been annealed significantly, TK-3 and TK-2 have been annealed slightly, and that TK-1 has been annealed minimally.

The age of the oldest fission tracks and the pooled fission-track age both generally increase up section (fig. 5). The age of the oldest tracks ranges from 5.5 to 15.0 Ma in samples TK-7 through TK-5, increases slightly to 18.8 Ma in TK-4, and increases more substantially to 50.3 Ma in TK-3 (the younger of two inferred populations) and to 61.1 Ma in TK-2 (fig. 5). The pooled AFT age, which closely tracks the oldest track age (fig. 5), suggests that cooling continued at least until the latest Tertiary (≈6–4 Ma; table 2). A second, older population (130 Ma) in TK-3 and two inferred populations in TK-1 (130 and 140 Ma) are interpreted to represent tracks formed during uplift of the provenance terrane, sediment dispersal, and deposition (fig. 5).

Time-temperature modeling of Topagoruk samples suggests a relatively simple Cenozoic cooling history. The t-T model for TK-1 provides limited insights regarding Cenozoic cooling because both inferred AFT populations (oldest tracks 130 and 140 Ma) predominately reflect cooling of the provenance terrane. Nevertheless, the t-T model for TK-1 suggests initiation of cooling about 75–65 Ma followed by monotonic cooling to the Quaternary (plate1).

The t-T models for TK-2 and TK-3 suggest an approximately monotonic cooling history throughout the Tertiary (plate 1). The ages of the oldest tracks are 61.1 Ma in TK-2 and 50.3 Ma in TK-3 (table 1, fig. 5); these tracks would have formed on the gradual cooling trajectory that began about 75–65 Ma. Pooled AFT ages of 51.7 Ma in TK-2 and 37.3 Ma in TK-3 suggest that cooling continued through the early Tertiary.

The t-T model for TK-4 suggests stable temperatures to very gradual cooling during the Early Tertiary followed by accelerated cooling starting about 35 Ma (plate 1). However, the envelope of statistically good model paths is quite broad between 35 and 20 Ma, so the accelerated cooling could have started at any time within that interval. Based on these model results, the oldest fission track (18.8 Ma) would have formed on the accelerated cooling trajectory that began about 35–20 Ma and continued until at least 11.7 Ma, as indicated by the pooled AFT age (table 2, fig. 5). The envelope of statistically good model paths for TK-4 is very broad between 65 and 35 Ma (plate. 1), so a variety of t-T trajectories is possible during the Early Tertiary.

The t-T models for TK-5 and TK-7 suggest stable temperatures to very gradual cooling during much of the Tertiary followed by accelerated cooling starting between 20 and 15 Ma (plate 1). The oldest tracks in these samples, 9.0 Ma in TK-5 and 5.5 Ma in TK-7, would have formed on this accelerated cooling trajectory that began in the Miocene. As with TK-4, the envelope of statistically good model paths is very broad between 65 and 20 Ma, so a variety of t-T trajectories is possible. The t-T model for TK-6 did not produce any statistically good fits to the measured AFT length data, although an envelope of statistically acceptable fits was achieved (plate. 1). This result would accommodate either a monotonic cooling throughout the Tertiary, or a t-T trajectory similar to that inferred for TK-5 and TK-7. Pooled AFT ages for these three samples suggest cooling continued into the latest Tertiary (6–4 Ma; table 2).

Note that the t-T models for TK-1 and TK-2 include a minimum temperature constraint during the Quaternary, which requires an increase in temperature to reach current conditions (plate 1). The use of the minimum temperature constraint, which was defined using the forward modeling capability in HeFTy, substantially increases the number of model paths that are statistically good or acceptable fits to the measured AFT length distributions.

Vitrinite reflectance values calculated using the "Easy $\%R_o$" kinetics of Sweeney and Burnham (1990) compare favorably with values derived from measured vitrinite reflectance for TK-2 through TK-6 (table 4; plate 1). Modeled vitrinite reflectance is significantly lower than the value derived from empirical data for TK-1, perhaps an indication that the empirical data include recycled vitrinite, as suggested for many data sets from North Slope well samples by Houseknecht and Hayba (1999) and Houseknecht and others (in press). Modeled vitrinite reflectance for TK-7 is higher than the value measured from the nearest sample, but it lies within the range of values (1.07–1.50 percent) measured over a 300 ft depth interval of basement strata (table 4; Johnsson and others, 1999). This observation and the favorable comparison for five other samples provide corroboration that the t-T models are reasonable approximations of the thermal history of those samples.

Ikpikpuk No. 1

Ikpikpuk is on the eastern flank of the northern NPRA uplift in an area where Bird (1988) estimated less than 1,000 ft of Nanushuk erosion (fig. 2). Ikpikpuk is in an area of moderate heat flow, as estimated by regional analysis (Deming and others, 1992, 1996). Samples range in stratigraphic position from the Triassic Ivishak Formation, at 10,776 ft subsea and a vitrinite reflectance of 1.3 percent, to the Lower Cretaceous Nanushuk Formation, at 2,881 ft subsea and a vitrinite reflectance of 0.5 percent (table 1).

Sample IK-6 currently is near the total AFT annealing threshold, samples IK-5 and IK-4 are at temperatures within the partial AFT annealing window, IK-3 is at a temperature slightly below the threshold of partial annealing, and IK-2 and IK-1 are at temperatures clearly lower than the threshold of partial annealing (fig. 4). Samples IK-6 and IK-5 contain few tracks, and all other samples contain abundant tracks (fig. 4). Mean track length increases consistently up section (fig. 4). These observations suggest that samples IK-6 and IK-5 have been annealed significantly, and that the degree of annealing in IK-4 through IK-1 grades from slight to minimal up section.

The age of the oldest fission tracks and the pooled fission-track age both increase up section (fig. 5). The age of the oldest tracks increases from 1.9 to 32.3 Ma over 542 ft of stratigraphic section from IK-6 to IK-5, then increases modestly over 3,148 ft of section to 46.8 Ma in IK-4 (fig. 5). The oldest fission tracks in all shallower samples range between 105 and 144 Ma (including two inferred populations in each of IK-2 and IK-1) and are interpreted to represent tracks formed during uplift of the provenance terrane, sediment dispersal, and deposition (fig. 5). The pooled AFT age of 65 Ma for IK-3 (table 2, fig. 5) likely reflects the initiation of uplift in the latest Cretaceous or earliest Tertiary.

Time-temperature modeling of Ikpikpuk suggests a Cenozoic cooling history similar to that of Topagoruk. The t-T models for IK-1 through IK-3 are influenced by the retention of AFT populations that reflect cooling of the provenance terrane or formation during deposition or shallow burial; that is, the AFT populations were not completely annealed during Brookian burial (table 1, fig. 5, plate. 1). Nevertheless, all three models suggest initiation of cooling about 75–65 Ma followed by monotonic cooling until the Quaternary (plate 1). Alternatively, there may have been a rapid rate of cooling until about 55 Ma followed by a slow rate of cooling until the Quaternary, as suggested by a subtle dogleg in the t-T models from all three samples (plate 1).

The t-T model for IK-4 suggests an approximately monotonic cooling history throughout the Tertiary (plate 1), although the envelope of statistically good model paths is very broad prior to 55 Ma, so a variety of t-T trajectories is possible during the Early Tertiary.

The t-T models for IK-5 and IK-6 suggest stable temperatures to gradual cooling during much of the Tertiary followed by accelerated cooling starting between 20 and 15 Ma (plate 1). The oldest track inferred in IK-5 (32.3 Ma) would have formed during the gradual cooling trajectory, and the oldest track inferred in IK-6 (1.9 Ma) would have formed during the accelerated cooling trajectory. The pooled AFT age of 15.2 Ma for IK-5 likely reflects the accelerated cooling. These interpretations are tentative because the t-T model for IK-5 did not produce any statistically good fits to the measured AFT length data, although an envelope of statistically acceptable fits was achieved, and the t-T model for IK-6 includes a very broad envelope of statistically good fits prior to 20–15 Ma. Therefore, a variety of t-T trajectories is possible for both samples.

Note that the t-T models for IK-1 through IK-4 include a minimum temperature constraint during the Quaternary, which requires an abrupt increase in temperature to reach current conditions (plate 1). The use of the minimum temperature constraint, which was defined using the forward modeling capability in HeFTy, substantially increases the number of model paths that are statistically good or acceptable fits to the measured AFT length distributions.

Vitrinite reflectance values calculated using the "Easy $\%R_o$" kinetics of Sweeney and Burnham (1990) compare favorably with values derived from measured vitrinite reflectance for most t-T models (table 4; plate 1). The largest differences occur in IK-1, IK-2, and IK-5. The differences in IK-1 and IK-2 may be the result of recycled vitrinite in the empirical data set, and no explanation can be offered for the difference in IK-5. Nevertheless, the favorable comparison for the other samples provides corroboration that the t-T models are reasonable approximations of the thermal history of those samples.

Summary of Time-Temperature Histories of the Three Wells

The results presented in preceding sections indicate that the post-LCU thermal histories of South Meade, Topagoruk, and Ikpikpuk include burial to maximum temperature in the latest Cretaceous or earliest Tertiary followed by significant cooling during the Tertiary and, perhaps, reheating during the Quaternary. There are, however, important contrasts in thermal history among the three locations.

South Meade t-T models indicate 100–140°C of total cooling that began 75–65 Ma and culminated during the latest Tertiary or Quaternary (plate 1). This cooling does not appear to have been monotonic throughout the Tertiary. Rather, the rate of cooling appears to have been moderate (average rate 1–2°C/my) during the early Tertiary and more rapid during the late Tertiary (average rate 3–6°C/my; plate 1). This bimodal cooling history suggests two distinct pulses of uplift and erosion, the first beginning in the latest Cretaceous or earliest Tertiary (75–65 Ma) and the second beginning in the late Paleogene or early Neogene (35–15 Ma). Cooling continued until at least the latest Miocene (7–5 Ma). The t-T model for each South Meade sample suggests significant (40–80°C) reheating during the Quaternary (plate 1). In the absence of any geological data that indicate a recent increase in burial depth, this reheating most likely reflects a recent increase in heat flow, although perturbation of the subsurface thermal regime resulting from the insulating effect of abrupt permafrost development (Carter and Hillhouse, 1992) may have been a contributing factor.

Topagoruk t-T models indicate 50–80°C of total cooling that began 75–65 Ma and culminated during the latest Tertiary or Quaternary (plate 1). The t-T models for TK-1 through TK-3 and TK-6 suggest monotonic cooling throughout the Tertiary, and the models for TK-4, TK-5, and TK-7 suggest accelerated cooling that started 35–15 Ma (plate 1). Cooling continued until at least the latest Miocene (6–4 Ma). Average rates of cooling are estimated to have been 0.7–1.4°C/my during the early Tertiary, perhaps increasing to 1.5–3°C/my during the late Tertiary.

Ikpikpuk t-T models indicate 40–70°C of total cooling that began 75–65 Ma and culminated no earlier than the late Tertiary (plate 1). Most models suggest monotonic cooling throughout the Tertiary, although the models for IK-5 and IK-6 display subtle suggestions of accelerated cooling that started 20–15 Ma (plate 1). Cooling continued until at least the middle Miocene (15.2 Ma). Average rates of cooling are estimated to have been 0.5–1.2°C/my. In general, these observations suggest gradual uplift and erosion extending through the Tertiary Period.

The t-T models for two samples in Topagoruk and four samples in Ikpikpuk suggest 10–30°C of increased temperature during the Quaternary (plate 1). Unlike South Meade, the subtle evidence of this reheating event is not observed in the deepest samples, so increased heat flow is not a viable explanation. Therefore, we tentatively suggest that perturbation of the subsurface thermal regime resulting from the insulating effect of abrupt permafrost development may be responsible.

Magnitude of Uplift and Erosion

Assuming that the amount of Tertiary cooling estimated for the three wells is entirely or mostly the consequence of uplift and erosion, estimates of the magnitude of exhumation can be made for each location. Considering the range of cooling estimated for each well (cited above) and a range of thermal gradients around the current gradient (table 1), the AFT analysis suggests exhumation of 5,500–8,000 ft at South Meade, 4,000–8,000 ft at Topagoruk, and 3,000–6,500 ft at Ikpikpuk.

Discussion

Although AFT analysis provides certain constraints on the absolute magnitude of uplift and erosion (for example, Gleadow and others, 1986; O'Sullivan, 1999; Dumitru, 2000; Donelick and others, 2005), inferences derived from this method commonly are constrained by estimates of geothermal gradient and various measures of thermal maturity (for example, vitrinite reflectance). Recent modeling of the thermal maturation history of more than 100 exploration wells, however, indicates that vitrinite reflectance is not in equilibrium with current heat flow across much of Arctic Alaska (Houseknecht and others, in press). Moreover, the suggestion that heat flow may have increased significantly during the Quaternary at South Meade calls into question the use of the current geothermal gradient to estimate the magnitude of uplift and erosion that occurred earlier in the Cenozoic. The following discussion, therefore, summarizes estimates of uplift and erosion determined by a variety of independent techniques.

The absolute amount of uplift and erosion at the South Meade, Topagoruk, and Ikpikpuk well sites can be estimated by considering regional stratigraphic information (Bird, 1988), uplift estimates derived from sonic log compaction curves (Nelson and Bird, 2005; Burns and others, 2007), thermal maturity data, and results of thermal maturation modeling (Houseknecht and others, in press). Well data in eastern NPRA and the Colville River delta (fig. 2) indicate the presence of about 3,500 ft of Upper Cretaceous strata below the basal Paleogene unconformity (fig. 1). Moreover, well and seismic data indicate that Upper Cretaceous strata thin gradually westward. It is reasonable to assume, therefore, that 2,000–3,500 ft of Upper Cretaceous strata were deposited above the Nanushuk Formation across northern NPRA. Adding this range of Upper Cretaceous stratal thickness to Bird's (1988) estimates of Nanushuk Formation eroded at each location yields total exhumation estimates of 5,000–6,500 ft at South Meade, 4,000–5,500 ft at Topagoruk, and 2,500–4,000 ft at Ikpikpuk. These ranges would increase if Lower Tertiary strata also were deposited across the region.

Erosion estimates based on compaction curves derived from sonic logs from exploration wells using two different

analytical techniques have been published for the South Meade and Ikpikpuk wells; no estimate is available for Topagoruk as no sonic log exists for that well. Estimates of the magnitude of erosion by Nelson and Bird (2005) are 4,800 ft at South Meade and at least 4,200 ft at Ikpikpuk. Estimates of exhumation by Burns and others (2007) are 3,350 ft at South Meade and 2,325 ft at Ikpikpuk.

Nelson and Bird (2005) also estimated the amount of erosion at various locations in NPRA using depth versus vitrinite reflectance plots (essentially the method of Dow, 1977). Although the three wells analyzed in this report were not included in their study, they estimated that the amount of erosion increases from about 1,000 ft in northeastern NPRA (west of the Colville River delta) to nearly 7,000 ft in northwestern NPRA between Point Barrow and Peard Bay (fig. 2). Burns and others (2007) also used depth versus vitrinite reflectance data and the Dow (1977) technique to estimate erosion magnitudes of 3,700 ft at South Meade, 5,500 ft at Topagoruk, and 2,300 ft at Ikpikpuk.

Unpublished thermal maturity data from coal beds in the Wainwright No. 1 (figs. 1 and 2)—a continuously cored, 1,600-ft deep borehole drilled to test coal-bed gas potential in the Nanushuk Formation—indicate that mean vitrinite reflectance is about 0.5 percent from the surface to total depth. Application of depth versus vitrinite reflectance gradients from three nearby wells—Peard, Kugrua, and Tunalik (figs. 1 and 2)—results in an estimate of 3,000–7,000 ft of exhumation at Wainwright. The uncertainty in this estimate stems from substantial differences in the slope of depth versus log vitrinite reflectance plots among the three reference wells. The "Easy $\%R_o$" (Sweeney and Burnham, 1990) method suggests 6,000–8,000 ft of exhumation at Wainwright for a 40–30°C/km range of geothermal gradients.

Erosion amounts derived from thermal maturation modeling of all wells in NPRA using estimated values of heat-flow and thermal conductivity through geologic time (Houseknecht and others, in press) are >4,000 ft at South Meade, >3,500 ft at Topagoruk, and >2,500 ft at Ikpikpuk. Although this modeling utilized depth versus vitrinite reflectance trends as a constraint, it relied primarily on kinetic calculations and analysis of lateral variability in heat-flow data.

Results from all the techniques summarized above consistently indicate a pattern of increased uplift and erosion towards the northwestern coast of NPRA, but estimates of the magnitude of exhumation vary considerably. On a regional basis, these diverse techniques indicate minimal exhumation in the Colville River delta increasing northwestward to perhaps as much as 7,000 ft or more of exhumation along the coast between Point Barrow and Peard Bay. Within this regional context, and considering the inherent uncertainty associated with the techniques summarized above, it is likely that the magnitude of exhumation resulting from Tertiary uplift and erosion at the three well locations ranges from 2,500–4,000 ft at Ikpikpuk, 4,000–5,500 ft at Topagoruk, and 5,000–6,500 ft at South Meade. The new AFT data and interpretations reported in this paper overlap (on the high side) with these ranges of exhumation.

Even though the work presented here provides documentation of the overall geometry, timing, and magnitude of the northern NPRA uplift, it does not address the geologic origin of the uplift. That topic is beyond the scope of this effort and awaits completion of additional research.

Conclusions

Regional truncation of Cretaceous strata beneath a Pliocene unconformity, lateral trends in thermal maturity defined by vitrinite reflectance data, and a pattern of exhumation estimated from analysis of sonic logs from exploration wells define a broad, post-mid-Cretaceous uplift in northern NPRA. AFT analysis of core samples from the South Meade, Topagoruk, and Ikpikpuk exploration wells, which traverse the eastern flank of the uplift, indicates significant cooling during the Tertiary followed by local increases in temperature.

AFT data from South Meade indicate uplift and erosion starting about 75–65 Ma (latest Cretaceous–earliest Tertiary) and extending throughout the Tertiary Period, with an acceleration of exhumation starting about 35–15 Ma (latest Eocene–middle Miocene). A significant increase in temperature during the Quaternary also is indicated. The Quaternary increase in temperature is interpreted as being the result of increased heat flow, although the insulating effect of abrupt permafrost development may have contributed to subsurface temperature perturbations.

AFT data from Topagoruk and Ikpikpuk similarly indicate uplift and erosion starting about 75–65 Ma and extending throughout the Tertiary Period. Topagoruk data include evidence suggesting accelerated exhumation starting about 35–20 Ma, and Ikpikpuk data include subtle evidence suggesting accelerated exhumation starting about 20–15 Ma. The suggestion of a Quaternary temperature increase is revealed in the t-T models of some samples from Topagoruk and Ikpukpuk but, because this evidence is lacking in the deepest samples from both wells, it is interpreted to reflect subsurface temperature perturbation caused by the insulating effect of abrupt permafrost development rather than an increase in heat flow.

Estimates of the magnitude of uplift in northern NPRA vary substantially among geological parameters used for analysis. Compaction curves derived from sonic logs tend to yield relatively low estimates, reconstruction of regional stratigraphy yields relatively high estimates, and thermal maturity data yield a range of estimates that spans values from the other techniques. The AFT data reported here yield estimates of exhumation that are among the highest of any technique. Considering the inherent variability and uncertainty associated with the different datasets, we estimate the magnitude of exhumation resulting from uplift and erosion to be 5,000–6,500 ft at South Meade, 4,000–5,500 ft at Topagoruk, and 2,500–4,000 ft at Ikpikpuk.

References

Bergman, S.C., Decker, J., Kelley, S., and Talbot, J., 1991, Apatite and zircon fission track analyses of nine selected wells in the NPRA, Alaska: Alaska Geologic Materials Center Data Report 189, 52 p., http://www.dggs.alaska.gov/webpubs/dggs/gmc/text/gmc189.PDF (last accessed April 9, 2011).

Bird, K.J., 1988, Structure-contour and isopach maps of the National Petroleum Reserve in Alaska, *in* Gryc, G., ed., Geology and exploration of the National Petroleum Reserve in Alaska, 1974 to 1982: U.S. Geological Survey Professional Paper 1399, p. 355–377.

Burns, W.M., Hayba, D.O., Rowan, E.L., and Houseknecht, D.W., 2007, Estimating the amount of eroded section in a partially exhumed basin using geophysical logs—An example from the Alaska North Slope: U.S. Geological Survey Professional Paper 1732–D, 18 p., http://pubs.usgs.gov/pp/pp1732/pp1732d/ (last accessed April 9, 2011).

Carlson, W.D., Donelick, R.A., and Ketcham, R.A., 1999, Variability of apatite fission-track annealing kinetics, I—Experimental results: American Mineralogist, v. 84, p. 1213–1223.

Carter, L. D., and Hillhouse, J.W., 1992, Age of the Late Cenozoic Bigbendian marine transgression of the Alaskan Arctic coastal plain—Significance for permafrost history and paleoclimate, *in* Bradley, D. C., and Ford, A.B., eds., U.S. Geological Survey Bulletin 1999, p. 44–51.

Coakley, B.J., and Watts, A.B., 1991, Tectonic controls on the development of unconformities—The North Slope, Alaska: Tectonics, v. 10, p. 101–130.

Deming, D., Sass, J.H., and Lachenbruch, A.H., 1996, Heat flow and subsurface temperature, North Slope of Alaska, *in* Johnsson, M.J., and Howell, D.G., eds., Thermal evolution of sedimentary basins in Alaska: U.S. Geological Survey Bulletin 2142, p. 21–44.

Deming, D., Sass, J.H., Lachenbruch, A.H., and DeRito, R.F., 1992, Heat flow and subsurface temperature as evidence for basin-scale ground-water flow, North Slope of Alaska: Geological Society of America, v. 104, p. 528–542.

Donelick, R.A., Ketcham, R.A., and Carlson, W.D., 1999, Variability of apatite fission-track annealing kinetics, II—Crystallographic orientation effects: American Mineralogist, v. 84, p. 1224–1234.

Donelick, R.A., O'Sullivan, P.B., and Ketcham, R.A., 2005, Apatite fission-track analysis: Reviews in Mineralogy and Geochemistry, v. 58, p. 49–94.

Dow, W.G., 1977, Kerogen studies and geological interpretations: Journal of Geochemical Exploration, v. 7, p. 79–99.

Dumitru, T.A., 2000, Fission-track geochronology, *in* Quaternary geochronology; methods and applications: AGU Reference Shelf, v. 4, p. 131–155.

Gallagher, K., Brown, R., and Johnson, C., 1998, Fission track analysis and its applications to geological problems: Annual Reviews of Earth and Planetary Science, v. 26, p. 519–572.

Gleadow, A.J.W., Duddy, I.R., Green, P.F., and Lovering, J.F., 1986, Confined fission track lengths in apatite—A diagnostic tool for thermal history analysis: Contributions to Mineral Petrology, v. 94, p. 405–415.

Houseknecht, D.W., and Bird, K.J., 2004, Sequence stratigraphy of the Kingak Shale (Jurassic–Lower Cretaceous), National Petroleum Reserve in Alaska: American Association of Petroleum Geologists Bulletin, v. 88, p. 279–302.

Houseknecht, D.W., and Bird, K.J., 2011, Geology and petroleum potential of the rifted margins of the Canada basin, *in* Spencer, A., Gautier, D., Sørensen, K., Stoupakova, A., and Embry, A., eds., Arctic petroleum geology: Geological Society of London Memoir 35, p. 509–526.

Houseknecht, D.W., and Hayba, D.O., 1999, Modeling oil generation in the undeformed part of the Arctic National Wildlife Refuge 1002 Area, *in* Takahashi, K.I., and Nelson, P.H., eds., The Oil and Gas Resource Potential of the Arctic National Wildlife Refuge 1002 Area, Alaska: U.S. Geological Survey Open-File Report 98-34, 45 p., http://energy.cr.usgs.gov/OF98-34/HG.pdf (last accessed April 9, 2011).

Houseknecht, D.W., Bird, K.J., and Schenk, C.J., 2009, Seismic analysis of clinoform depositional sequences and shelf-margin trajectories in Albian strata, Alaska North Slope: Basin Research, v. 21, p. 644–654.

Houseknecht, D.W., Bird, K.J., Schuenemeyer, J.H., Attanasi, E.D., Garrity, C.P., Schenk, C.J., Charpentier, R.R., Pollastro, R.M., Cook, T.A., and Klett, T.R., 2010, 2010 updated assessment of undiscovered oil and gas resources of the National Petroleum Reserve in Alaska (NPRA): U.S. Geological Survey Fact Sheet 2010–3102, 4 p., http://pubs.usgs.gov/fs/2010/3102/pdf/FS10-3102.pdf (last accessed April 9, 2011).

Houseknecht, D.W., Burns, W.M., and Bird, K.J., in press, Thermal maturation history of Arctic Alaska and southern Canada basin: *in* Harris, N.B., and Peters, K.E., eds., Thermal History of Sedimentary Basins: SEPM Special Publication.

Hubbard, R.J., Edrich, S.P., and Rattey, R.P., 1987, Geologic evolution and hydrocarbon habitat of the "Arctic Alaska microplate": Marine and Petroleum Geology, v. 4, no. 1, p. 2–34.

Johnsson, M.J., Evans, K.R., and Marshall, H.A., 1999, Thermal maturity of sedimentary rocks in Alaska: Digital

Resources: U.S. Geological Survey, Digital Data Series DDS-54, http://pubs.usgs.gov/dds/dds-54/ (last accessed April 9, 2011).

Johnsson, M.J., Howell, D.G., and Bird, K.J., 1993, Thermal maturity patterns in Alaska: Implications for tectonic evolution and hydrocarbon potential: American Association of Petroleum Geologists Bulletin, v. 77, p. 1874–1903.

Ketcham, R.A., 2005, Forward and inverse modeling of low-temperature thermochronometry data: Reviews in Mineralogy and Geochemistry, v. 58, p. 275–314.

Ketcham, R.A., Donelick, R.A., and Carlson, W.D., 1999, Variability of apatite fission-track annealing kinetics, III—Extrapolation to geological time scales: American Mineralogist, v. 84, p. 1235–1255.

Ketcham, R.A., Carter, A., Donelick, R.A., Barbarand, J., and Hurford, A.J., 2007, Improved modeling of fission-track annealing in apatite: American Mineralogist, v. 92, p. 799–810.

Lachenbruch, A.H., Sass, J.H., Lawver, L.A., Brewer, M.C., Marshall, B.V., Munroe, R.J., Kennelly, J.P., Jr., Galanis, S.P., Jr., and Moses, T.H., Jr., 1988, Temperature and depth of permafrost on the Arctic slope of Alaska, *in* Gryc, G., ed., Geology and exploration of the National Petroleum Reserve in Alaska, 1974 to 1982: U.S. Geological Survey Professional Paper 1399, p. 645–656.

Moore, T.E., Potter, C.J., O'Sullivan, P.B., Shelton, K.L., and Underwood, M.B., 2004, Two stages of deformation and fluid migration in the west-central Brooks Range fold-and-thrust belt, northern Alaska, *in* Swennen, R., Roure, F., and Granath, J., eds., Deformation, fluid flow and reservoir appraisal in foreland fold-and-thrust belts: American Association Petroleum Geologists Hedberg Series, no. 1, p. 157–186.

Moore, T.E., Wallace, W.K., Bird, K.J., Karl, S.M., Mull, C.G., and Dillon, J.T., 1994, Geology of northern Alaska, *in* Plafker, G., and Berg, H.C., eds., The geology of Alaska: Boulder, Colorado, Geological Society of America, The geology of North America, v. G-1, p. 49–140.

Mull, C.G., Houseknecht, D.W., and Bird, K.J., 2003, Revised Cretaceous and Tertiary stratigraphic nomenclature in the east-central Colville basin, northern Alaska: U.S. Geological Survey Professional Paper 1673, pubs.usgs.gov/prof/p1673 (last accessed April 9, 2011).

Murphy, J.M., 1994, Apatite fission track data derived from core from four Barrow arch wells: Alaska Geologic Materials Center Data Report 220, 10 p., http://www.dggs.alaska.gov/webpubs/dggs/gmc/text/gmc220.PDF (last accessed April 9, 2011).

Nelson, P.H., and Bird, K.J., 2005, Porosity-depth trends and regional uplift calculated from sonic logs, National Petroleum Reserve in Alaska: U.S. Geological Survey Scientific Investigations Report 2005–5051, 23 p.

Nunn, J.A., Czerniak, M., and Pilger, R.H., Jr., 1987, Constraints on the structure of Brooks Range and Colville Basin, northern Alaska, from flexure and gravity analysis: Tectonics, v. 6, p. 603–617.

O'Sullivan, P.B., 1993, Late Cretaceous and Tertiary thermal and uplift history of the North Slope foreland basin of northern Alaska and northwestern Canada: LaTrobe University, Melbourne, Australia, Ph.D. dissertation, 419 p.

O'Sullivan, P.B., 1996, Late Mesozoic and Cenozoic thermal-tectonic evolution of the North Slope foreland basin, Alaska, *in* Johnsson, M.J., and Howell, D.G., eds., Thermal evolution of sedimentary basins in Alaska: U.S. Geological Survey Bulletin, 2142, p. 45–79.

O'Sullivan, P.B., 1999, Thermochronology, denudation and variations in palaeosurface temperature: A case study from the North Slope foreland basin, Alaska: Basin Research, v. 11, p. 191–204.

Sweeney, J.J., and Burnham, A.K., 1990, Evaluation of a simple model of vitrinite reflectance based on chemical kinetics: American Association of Petroleum Geologists Bulletin, v. 64, p. 1559-1570.

Walker, J.D., and Geissman, J.W., 2009, Geologic time scale: Geological Society of America, 1 p., http://www.geosociety.org/science/timescale/ (last accessed April 9, 2011).

This page left blank intentionally.

Tables 1–4

Table 1. Basic information regarding wells, samples, and apatite fission-track analysis, National Petroleum Reserve in Alaska.

[GE, ground elevation; KB, kelly bushing elevation; current temperature estimated from approximate thermal gradient; vitrinite reflectance estimated at midpoint of sample depth interval using data from Johnsson and others (1999); data quality expressed on scale from 1, poor to 10, excellent; *D*par, criterion used to infer whether one or multiple populations are present in measured fission track distribution (Donelick and others, 2005)]

Well	Elevation in feet and thermal gradient	USGS sample number	Sample depth interval in feet	Sample midpoint depth in feet	Sample midpoint elevation in feet	Formation	Current temperature in °C	Vitrinite reflectance in percent	Apatite grains observed	Data quality	*D* par of oldest track in µm	Age of oldest fission track in Ma
South Meade #1	GE: 40 KB: 60 52°C/km	SM-1	3,015–3,020	3,018	-2,958	Torok	35	0.60	100s	6	1.60; 2.20	78.5 ± 6.3; 108 ± 34.7
		SM-2	5,995–5,998	5,997	-5,937	Torok	82	0.84	100s	7	1.74	26.1 ± 2.8
		SM-3	8,508–8,512	8,510	-8,450	Kingak	122	2.09	100s	4	1.48	23.5 ± 3.5
		SM-4	8,819–8,821	8,820	-8,760	Sag River	127	2.15	100s	2	1.59	12.7 ± 5.1
		SM-5	9,049–9,054	9,052	-8,992	Shublik	130	2.19	10s	2	1.65	15.1 ± 15.1
		SM-6	9,309–9,315	9,313	-9,253	Ivishak	135	2.28	100s	2	1.75	0.0 ± 0.0
Topagoruk #1	GE: 28 KB: 42 32°C/km	TK-1	2,090–2,095	2,093	-2,051	Nanushuk	12	0.47	1000s	6	1.63; 2.15	130 ± 8.3; 140 ± 19.2
		TK-2	5,970–5,990	5,980	-5,938	Torok	50	0.68	1000s	7	1.66	61.1 ± 4.5
		TK-3	6,500–6,510	6,505	-6,463	Torok	55	0.78	1000s	7	1.65;2.38	50.3 ± 4.2; 130 ± 27.5
		TK-4	7,829–7,839	7,834	-7,792	Kingak	68	0.84	10s	5	1.73	18.8 ± 4.6
		TK-5	9,441–9,443	9,442	-9,400	Ivishak	83	0.98	100s	4	1.76	9.0 ± 1.4
		TK-6	9,573–9,575	9,574	-9,532	Ivishak	85	1.02	10s	3	1.89	15.0 ± 4.7
		TK-7	10,228–10,229	10,229	-10,187	basement	92	[1]1.19	10s	3	1.67	5.5 ± 3.2
Ikpikpuk #1	GE: 32 KB: 52 36°C/km	IK-1	2,930–2,935	2,933	-2,881	Nanushuk	17	0.52	1000s	6	1.75; 2.67	105 ± 7.0; 108 ± 34.4
		IK-2	3,785–3,790	3,788	-3,736	Torok	27	0.55	100s	7	1.64; 2.21	140 ± 7.9; 144 ± 22.4
		IK-3	5,690–5,700	5,695	-5,643	Torok	48	0.60	1000s	6	1.72	111 ± 7.9
		IK-4	7,133–7,143	7,138	-7,086	Torok	64	0.70	1000s	6	1.73	46.8 ± 3.7
		IK-5	10,283–10,289	10,286	-10,234	Shublik	99	1.20	10s	5	1.88	32.3 ± 9.4
		IK-6	10,825–10,830	10,828	-10,776	Ivishak	105	1.32	1000s	7	1.52	1.9 ± 0.4

[1]Measured mean value near AFT sample—four measurements in basement rocks are highly variable between 1.07 and 1.50 percent.

Table 2. Data derived from apatite fission-track analysis of standards and samples from three wells in the northern National Petroleum Reserve in Alaska.

[These data were used for analytical quality control and age interpretation as described by Donelick and others (2005). Dpar, diameter of etch figure parallel to the crystallographic c axis; Dper, mean maximum diameter of fission-track etch figure perpendicular to the crystallographic c axis; N_S, number of spontaneous fission tracks over a selected grain area, which is used as a measure of track density; Σ(PΩ), sum of the 238U/43Ca ratios measured over the area Ω; 1σ Σ(PΩ), standard error of Σ(PΩ); ζ_{MS}, zeta calibration factor based on laser-ablation inductively coupled plasma-mass spectrometry of fission-track age standards adjusted for the sample position during analysis; 1σ ζ_{MS}, standard error of ζ_{MS}; bkg:sig, background to signal; dmnls, dimensionless; Q, Chi² probability]

	USGS sample number	Grains (dmnls)	*D* par in µm	*D* per in µm	N_s	Area analyzed in cm²	Σ(PΩ) in cm²	1σ(PΩ) in cm²	ζ_{MS}	1σ ζ_{MS}	^{43}Ca bkg:sig (dmnls)	^{238}U bkg:sig (dmnls)	Q (dmnls)	Pooled fission-track age in Ma
Age Standards														
Durango 30.6 ± 0.3 Ma		419	no data	no data	2222	1.97E-2	5.77E-4	4.47E-6	16.365	0.373	1.11E-1	1.10E-2		**31.4 ± 1.0**
Fish Canyon Tuff 27.51 ± 0.07 Ma		25	1.75	0.49	178	9.47E-4	3.86E-5	1.30E-6	13.114	0.298	5.34E-2	3.47E-3	0.981	**30.2 ± 2.6**
Apatite to Zircon, Inc., Age Standards (internal standards used by company that conducted the apatite fission-track analysis)														
Tioga Bed B ~220 Ma		25	1.79	0.49	2930	9.28E-4	8.59E-5	2.86E-6	13.245	0.301	4.59E-2	1.35E-3	0.383	**222 ± 10**
Mt. Dromedary 98.6 Ma		39	1.23	0.31	1169	1.40E-3	7.76E-5	2.23E-6	12.943	0.294	4.92E-2	2.80E-3	0.000	**96.8 ± 4.5**
Well														
South Meade #1	SM-1	40	1.62	0.44	234	7.02E-4	2.58E-5	9.71E-7	15.338	0.348	5.04E-2	9.12E-3	0	**69.2 ± 5.5**
	SM-2	39	1.67	0.44	211	1.08E-3	7.41E-5	5.75E-6	15.128	0.343	5.75E-2	2.53E+0	0	**21.5 ± 2.3**
	SM-3	26	1.60	0.41	53	3.81E-4	2.71E-5	1.52E-6	14.949	0.339	5.39E-2	4.06E+1	0.031	**14.6 ± 2.2**
	SM-4	27	1.55	0.46	6	2.39E-4	9.87E-6	4.52E-7	14.805	0.336	7.77E-2	1.49E+0	0.111	**4.50 ± 1.85**
	SM-5	12	1.61	0.49	1	1.55E-4	1.10E-6	7.33E-8	14.697	0.334	5.85E-2	2.49E-1	0.999	**6.68 ± 6.69**
	SM-6	29	1.75	0.44	0	3.99E-4	2.86E-5	1.91E-6	14.581	0.331	7.00E-2	2.79E-1	n.a.	**0.000 ± 0.382**
Topagoruk #1	TK-1	40	1.74	0.45	742	7.11E-4	4.63E-5	1.73E-6	14.398	0.327	5.01E-2	1.21E-2	0	**114 ± 7**
	TK-2	39	1.69	0.44	299	8.53E-4	4.09E-5	1.60E-6	14.188	0.322	5.25E-2	8.90E-3	0	**51.7 ± 3.8**
	TK-3	40	1.69	0.46	246	1.20E-3	4.60E-5	1.86E-6	13.977	0.318	5.26E-2	7.04E-3	0.191	**37.3 ± 2.9**
	TK-4	20	1.67	0.48	25	2.89E-4	1.48E-5	1.01E-6	13.815	0.314	5.01E-2	2.72E-2	0.853	**11.7 ± 2.5**
	TK-5	40	1.71	0.51	49	7.93E-4	5.67E-5	3.25E-6	13.652	0.310	5.14E-2	3.32E-2	0	**5.90 ± 0.92**
	TK-6	30	1.79	0.53	11	5.71E-4	1.55E-5	6.24E-7	13.468	0.306	4.80E-2	1.08E-2	0.336	**4.79 ± 1.46**
	TK-7	14	1.74	0.44	3	3.95E-4	5.02E-6	3.50E-7	13.350	0.304	5.13E-2	1.76E-2	0.801	**3.99 ± 2.32**
Ikpikpuk #1	IK-1	40	1.74	0.48	525	5.60E-4	4.61E-5	1.99E-6	16.485	0.374	4.63E-2	2.11E-2	0	**93.1 ± 6.1**
	IK-2	40	1.64	0.39	845	7.28E-4	5.51E-5	2.15E-6	16.267	0.369	4.73E-2	1.03E-2	0	**124 ± 7**
	IK-3	41	1.65	0.43	326	6.25E-4	4.00E-5	1.53E-6	16.047	0.364	4.83E-2	4.46E-3	0	**65.0 ± 4.6**
	IK-4	40	1.64	0.45	289	8.93E-4	6.22E-5	3.04E-6	15.831	0.359	5.18E-2	7.40E-3	0	**36.7 ± 2.9**
	IK-5	8	1.67	0.39	14	1.01E-4	7.24E-6	8.08E-7	15.690	0.356	5.04E-2	4.19E-3	0.002	**15.2 ± 4.4**
	IK-6	40	1.43	0.33	13	5.62E-4	2.05E-4	5.92E-6	15.548	0.353	4.80E-2	2.92E-2	0.946	**0.494 ± 0.138**

Table 3. Apatite fission-track frequency and length data for standards and samples from three wells in the northern National Petroleum Reserve in Alaska.

[*D*par, diameter of etch figure parallel to the crystallographic c axis; *D*per, mean maximum diameter of fission-track etch figure perpendicular to the crystallographic c axis; -, no tracks observed in this track-length class]

	USGS sample number	Number of tracks	Mean track length ± standard error in µm	Standard deviation of track length in µm	*D*par in µm	*D*per in µm	Number of fission-tracks measured in the following track-length classes																		
							0–1 µm	1–2 µm	2–3 µm	3–4 µm	4–5 µm	5–6 µm	6–7 µm	7–8 µm	8–9 µm	9–10 µm	10–11 µm	11–12 µm	12–13 µm	13–14 µm	14–15 µm	15–16 µm	16–17 µm	17–18 µm	18–19 µm	19–20 µm
Length Standards																									
Durango-D 31.4 Ma		138	**14.59 ± 0.08**	0.98	1.87	0.22	-	-	-	-	-	-	-	-	-	-	-	1	5	28	60	32	10	2	-	-
Fish Canyon Tuff-D 27.8 Ma		130	**15.01 ± 0.09**	1.02	2.36	0.46	-	-	-	-	-	-	-	-	-	-	-	1	3	16	46	39	23	2	-	-
Well																									
South Meade #1	SM-1	165	**13.51 ± 0.13**	1.65	1.66	0.40	-	-	-	-	-	-	-	-	2	2	3	23	30	39	36	18	10	2	-	-
	SM-2	94	**12.74 ± 0.19**	1.84	1.73	0.46	-	-	-	-	1	-	-	-	1	5	6	16	24	12	23	6	-	-	-	-
	SM-3	52	**10.72 ± 0.24**	1.69	1.65	0.42	-	-	-	-	-	1	1	1	6	5	13	13	10	2	-	-	-	-	-	-
	SM-4	19	**9.55 ± 0.40**	1.68	1.51	0.34	-	-	-	-	-	-	2	1	5	2	4	5	-	-	-	-	-	-	-	-
	SM-5	6	**9.47 ± 0.55**	1.23	1.29	0.40	-	-	-	-	-	-	-	-	3	1	1	1	-	-	-	-	-	-	-	-
	SM-6	3	**7.80 ± 0.47**	0.67	1.49	0.42	-	-	-	-	-	-	-	1	2	-	-	-	-	-	-	-	-	-	-	-
Topagoruk #1	TK-1	200	**13.55 ± 0.15**	2.06	1.68	0.40	-	-	-	-	1	1	2	1	2	7	9	8	24	46	59	29	9	2	-	-
	TK-2	125	**12.69 ± 0.16**	1.78	1.55	0.43	-	-	-	-	-	-	1	-	1	9	12	19	26	26	20	10	1	-	-	-
	TK-3	200	**11.36 ± 0.16**	2.19	1.72	0.43	-	-	-	1	1	1	7	7	11	21	32	26	49	20	21	2	1	-	-	-
	TK-4	31	**11.62 ± 0.35**	1.90	1.83	0.40	-	-	-	-	-	-	1	1	1	2	2	13	5	2	4	-	-	-	-	-
	TK-5	21	**9.96 ± 0.39**	1.74	1.79	0.59	-	-	-	-	-	-	1	3	3	3	4	5	2	-	-	-	-	-	-	-
	TK-6	23	**9.26 ± 0.41**	1.92	1.83	0.39	-	-	-	-	-	-	3	4	3	4	4	4	1	-	-	-	-	-	-	-
	TK-7	16	**11.07 ± 0.51**	1.96	1.53	0.33	-	-	-	-	-	-	-	-	1	6	2	3	-	3	1	-	-	-	-	-
Ikpikpuk #1	IK-1	200	**13.45 ± 0.12**	1.71	2.01	0.57	-	-	-	-	-	1	1	-	-	2	10	24	30	45	49	33	5	-	-	-
	IK-2	172	**12.66 ± 0.13**	1.73	1.89	0.55	-	-	-	-	-	-	-	1	5	9	18	22	36	35	38	7	1	-	-	-
	IK-3	160	**12.26 ± 0.13**	1.69	2.00	0.57	-	-	-	-	-	-	-	4	4	6	19	30	38	30	28	1	-	-	-	-
	IK-4	151	**11.90 ± 0.16**	1.97	2.00	0.59	-	-	-	-	-	-	1	3	7	12	26	24	32	29	8	4	5	-	-	-
	IK-5	31	**9.86 ± 0.24**	1.30	1.94	0.62	-	-	-	-	-	-	-	3	4	5	12	5	2	-	-	-	-	-	-	-
	IK-6	28	**9.77 ± 0.26**	1.37	1.71	0.37	-	-	-	-	-	-	-	3	4	9	4	8	-	-	-	-	-	-	-	-

Table 4. Age and temperature constraints used for inverse modeling of time-temperature history of each sample from three wells in the northern National Petroleum Reserve in Alaska.

[Each age (Ma) and temperature (°C) constraint is shown as a blue rectangle labeled with a letter in the time-temperature plots shown in plate 1; see text for additional explanation]

Sample	SM-6	SM-5	SM-4	SM-3	SM-2	SM-1	TK-7	TK-6	TK-5	TK-4	TK-3	TK-2	TK-1	IK-6	IK-5	IK-4	IK-3	IK-2	IK-1
Formation	Ivishak	Shublik	Sag River	Kingak	Torok	Torok	Basement	Ivishak	Ivishak	Kingak	Torok	Torok	Nanushuk	Ivishak	Shublik	Torok	Torok	Torok	Nanushuk
Provenance: source of apatite at elevated temperature ("P" in plate 1)																			
Age maximum in Ma	350	350	350	350	150	150	500	350	350	350	150	150	150	350	350	150	150	150	150
Age minimum in Ma	250	250	250	250	120	120	370	250	250	250	120	120	120	250	250	120	115	115	115
Temperature maximum in °C	220	220	220	220	220	220	220	220	220	220	220	220	220	220	220	220	220	220	220
Temperature minimum in °C	200	200	200	200	200	200	200	200	200	200	200	200	200	200	200	200	200	200	200
Deposition or exposure: sample strata at or near surface temperature ("D" and "X" in plate 1)																			
Age maximum in Ma	245	230	215	190	115	115	370	250	255	210	115	113	110	250	235	115	105	110	100
Age minimum in Ma	235	220	200	180	105	102	360	240	235	200	105	103	95	240	210	100	95	100	90
Temperature maximum in °C	20	20	20	20	20	20	20	20	20	20	20	15	20	20	20	20	20	20	20
Temperature minimum in °C	5	5	5	5	5	5	5	5	5	5	5	5	5	5	5	5	5	5	5
Neocomian burial to maximum temperature ("N" in plate 1)																			
Age maximum in Ma	136	136	136	136			136	136	136	136				136	136				
Age minimum in Ma	133	133	133	133			133	133	133	133				133	133				
Temperature maximum in °C	110	100	90	70			100	100	90	60				120	100				
Temperature minimum in °C	70	60	60	50			70	65	60	28.5				70	50				
Rift-shoulder uplift - LCU exhumation ("R" in plate 1)																			
Age maximum in Ma	133	133	133	133			133	133	133	133				133	133				
Age minimum in Ma	128	128	128	128			128	128	128	128				128	128				
Temperature maximum in °C	80	70	65	50			80	80	70	40				90	80				
Temperature minimum in °C	40	40	40	25			40	45	40	10				40	30				
Early Cretaceous burial ("E" in plate 1)																			
Age maximum in Ma	100	100	100	100	100	100	98	98	98	98	98	98	98	98	98	98	98	94	92
Age minimum in Ma	90	90	90	90	90	90	88	88	88	88	88	88	88	88	88	88	88	88	88
Temperature maximum in °C	160	160	150	120	110	90	160	140	140	130	115	110	60	170	150	110	90	80	50
Temperature minimum in °C	120	110	115	90	80	50	120	110	100	90	85	60	30	120	110	80	60	40	20
Late Cretaceous and earliest Tertiary burial ("T" in plate 1)																			
Age maximum in Ma	75	75	75	75	75	75	75	75	75	75	75	75	75	75	75	75	75	75	75
Age minimum in Ma	65	65	65	65	65	65	65	65	65	65	65	65	65	65	65	65	65	65	65
Temperature maximum in °C	180	200	190	180	160	125	210	180	170	150	125	120	70	200	200	150	115	90	80
Temperature minimum in °C	140	120	120	110	130	90	150	130	120	100	95	90	40	130	120	90	85	60	50

Table 4. Age and temperature constraints used for inverse modeling of time-temperature history of each sample from three wells in the northern National Petroleum Reserve in Alaska. —Continued

[Each age (Ma) and temperature (°C) constraint is shown as a blue rectangle labeled with a letter in the time-temperature plots shown in plate 1; see text for additional explanation]

Sample	SM-6	SM-5	SM-4	SM-3	SM-2	SM-1	TK-7	TK-6	TK-5	TK-4	TK-3	TK-2	TK-1	IK-6	IK-5	IK-4	IK-3	IK-2	IK-1
Formation	Ivishak	Shublik	Sag River	Kingak	Torok	Torok	Basement	Ivishak	Ivishak	Kingak	Torok	Torok	Nanushuk	Ivishak	Shublik	Torok	Torok	Torok	Nanushuk
Pliocene-Pleistocene low temperature ("L" in plate 1)																			
Age maximum in Ma	1	1	1	1	1	1						1	1			1	1	1	1
Age minimum in Ma	0.1	0.1	0.1	0.1	0.1	0.1						0.1	0.1			0.1	0.1	0.1	0.1
Temperature maximum in °C	100	70	50	40	35	20						40	15			55	45	25	15
Temperature minimum in °C	60	45	30	25	15	0						20	-10			35	25	10	0
Current temperature ("C" in plate 1)																			
Age maximum in Ma	0	0	0	0	0	0	0	0	0	0	0	0	0	0	0	0	0	0	0
Age minimum in Ma	0	0	0	0	0	0	0	0	0	0	0	0	0	0	0	0	0	0	0
Temperature maximum in °C	140	135	132	127	87	40	97	90	88	73	60	55	14	110	104	69	53	32	22
Temperature minimum in °C	130	125	122	117	77	30	87	80	78	63	50	45	7	100	94	59	43	22	12
Temperature current in °C	135	130	127	122	82	35	92	85	83	68	55	50	12	105	99	64	48	27	17
Vitrinite reflectance check																			
Modeled VR	2.26	2.19	2.14	1.85	0.94	0.68	1.41	1.01	1.04	0.85	0.74	0.65	0.21	1.32	1.37	0.71	0.61	0.47	0.43
Measured VR	2.28	2.19	2.15	2.09	0.84	0.60	(1)1.19	1.02	0.98	0.84	0.78	0.68	0.47	1.32	1.20	0.70	0.60	0.55	0.52

[1]Measured mean value near AFT sample—four measurements in basement rocks are highly variable between 1.07 and 1.50 percent.

Produced in Menlo Park, California
Manuscript approved for publication
April 14, 2011
Text edited by Tracey Suzuki
Layout and design by Judy Weathers